Materials Science-Poland, *Vol. 27*, *No. 1*, *2009*

The thermal stability, local structure and electrical properties of lithium-iron phosphate glasses

P. JÓŹWIAK[1] , J. E. GARBARCZYK[1*], M. WASIUCIONEK[1],
I. GORZKOWSKA[2], F. GENDRON[3], A. MAUGER[4], C. JULIEN[3]

[1]Faculty of Physics, Warsaw University of Technology, Koszykowa 75, 00-662 Warsaw, Poland

[2]Faculty of Chemistry, Warsaw University of Technology, Noakowskiego 3, 00-664 Warsaw, Poland

[3]Institut des Nanosciences de Paris, UMR-CNRS 7588, Université Pierre et Marie Curie,
140 rue de Lourmel, 75015 Paris, France

[4] Département MPPU, CNRS, Campus Boucicaut, 140 rue de Lourmel, 75015 Paris, France

Amorphous analogues of lithium-iron phosphates (LFP), which are promising cathode materials for Li ion batteries, were prepared by the standard press-quenching method and their thermal stability, as well as structural and electrical properties, were studied for the first time. The glass transition temperature, T_g, determined by the differential thermal analysis (DTA) is composition-dependent and lies in the 492–523 °C range. The local structure, studied by the FTIR absorption spectroscopy, and the thermal stability are found to be almost insensitive to the lithium content. Studies on the electrical properties, carried out by impedance spectroscopy, have shown that the total electrical (predominantly polaronic) conductivity at 450 °C approaches 10^{-2} S·cm^{-1}. The room temperature conductivity of samples after their nanocrystallization (induced by annealing at the temperature of the beginning of crystallization) was higher by a factor of 4–10 (depending on composition) than that of the as-received glass. Therefore, nanocrystallization seems to be a promising way to enhance the electrical conductivity of amorphous lithium-iron phosphates.

Key words: *phospho-olivines; lithium-iron phosphate; glasses; cathode material; nanomaterial; infrared spectroscopy; electron conduction*

1. Introduction

Crystalline olivine-type phases $LiFePO_4$ and $FePO_4$ as well as Li_xFePO_4 solid solutions are under intensive studies worldwide as the most competitive positive electrode-active materials for Li-ion rechargeable batteries. The main advantages of $LiFePO_4$ as a cathode material are that it is a highly stable, inexpensive and environmentally

*Corresponding author, e-mail: garbar@if.pw.edu.pl

friendly material which maintains high theoretical specific capacity of 170 mAh/g and a high discharge voltage of 3.5 V vs. Li [1–5]. Unfortunately, despite all their advantages, olivine-like phases have one serious deficiency – very low electrical (polaronic-type) conductivity - ca. 10^{-9} S·cm^{-1} at room temperature. Many efforts have been undertaken to improve their electrical properties by application of various routes of preparations: the introduction of carbon additives [5, 6], or by doping with supervalent cations [7]. Recently we proposed another, as yet unexplored, way of circumventing the problem of low conductivity of crystalline olivine cathode materials. As a first step we have prepared vitreous analogues of these materials and initiated studies on their local structure [8] and magnetic properties [9]. The second step, being currently under investigation, consists in turning these glasses into nanomaterials by an appropriate thermal treatment. In this respect, we took into consideration our recent experiences with mixed conductive lithium-vanadate phosphate glasses. We found that thermal nanocrystallization of those glasses results in a considerable enhancement of their electronic conductivity [10].

This work reports our most recent results of studies on the thermodynamic, structural and electric properties of lithium-iron-phosphate (LFP) glasses, whose nominal composition can be approximately written as Li_xFePO_4.

2. Experimental

A series of vitreous samples of (nominal composition) Li_xFePO_4 for $0 \le x \le 1$ were synthesized by a press quenching technique. Appropriate amounts of dried precursors: Li_2CO_3 (Aldrich, 99.99 %), $(NH_4)H_2PO_4$ (POCh, 99.5 %) and Fe_2O_3 (POCh, 99 %) were ground and mixed in a mortar. Alumina crucibles filled with the powders were placed in an electric furnace and heated from about 20 °C to 1270 °C in air at the heating rate of 5 °C/min. The molten mixtures kept at 1270 °C were rapidly poured out onto a stainless-steel plate maintained at the temperature close to 25 °C and immediately covered by a second stainless-steel plate. The average thickness of the resulting samples was 0.5–1.0 mm. Chemical analyses carried out by the inductive coupled plasma (ICP) method on the as-received samples have shown that due to evaporation of lithium during the high temperature stage of the synthesis, its content was slightly lower than the nominal one. For low values of x, the difference was negligible. Its maximum value for $x \approx 1$ reached 9%. The amorphous state of all as-quenched samples was confirmed by powder X-ray diffractometry (XRD), using a Philips X'Pert apparatus equipped with a $CuK_{\alpha 1}$ X-ray source and a Ni filter (λ = 1.54 Å). No Bragg peaks were detected in a wide range of 2θ angles between 10° and 80°. The thermal stability of the LFP glasses was studied by the differential thermal analysis (DTA). DTA runs were carried out for ground glass batches of about 130 mg in argon atmosphere at a heating rate 10 K·min^{-1} using a Perkin Elmer DTA-7 analyzer. The local structure of the samples was examined by the Fourier transform infra-red (FTIR) spectroscopy. FTIR absorption spectra of all glasses were recorded in the 150–1500 cm^{-1}

range at room temperature using a Bruker IFS 113v vacuum interferometer. For these measurements, each sample was ground to a fine powder, mixed with CsI in the ratio 1:300, and vacuum pressed into a disk. Electrical conductivity measurements were carried out using a setup based on a Solartron 1260 gain phase/impedance analyzer. The frequency range was 10 MHz–126 mHz. The measurements were carried out in air at temperatures, ranging from room temperature to the initial temperature of crystallization (533–558 °C, depending on composition). Prior to the impedance spectroscopy measurements, platinum electrodes were sputtered onto the opposite faces of the samples. The microstructure of partly recrystallized samples was observed by the field emission scanning electron microscopy (FE-SEM) using a LEO 1530 setup.

3. Results and discussion

3.1. Thermal stability and XRD studies

The differential thermal analysis curves for all glasses are shown in Fig. 1. Up to about 490 °C no thermal events are visible, which points to good thermal stability of the studied materials, especially in comparison with other conductive glasses. A typical run shows a glass transition feature (T_g) followed by an exothermic peak of crystallization, characterized by two parameters: T_{0c} (taken at the onset of the peak) and T_c (taken at the maximum). The first of them corresponds to the beginning of crystallization (nanocrystallization) and the second one corresponds to the end of crystallization (massive crystallization). The values of the glass transition temperature T_g are between 492 °C and 523 °C. The temperatures T_{0c} and T_c are in the 533– 558 °C and 555–579 °C ranges, respectively. A closer look at the asymmetric crystallization peaks reveals that they consist of at least two strongly overlapping peaks (Fig. 1) which are apparently due to different phases present in the crystallized material. Figure 2 shows room temperature XRD powder patterns for samples of three different compositions ($x = 0$, 0.4 and 1) taken after their crystallization. Two patterns are presented for the sample with $x = 0.4$. The upper one was taken after heating the sample up to T_{0c}, corresponding to beginning of crystallization (we refer to this sample as "nano"), and the lower one corresponds to the sample heated up to a temperature slightly above T_c, that means after massive crystallization (labelled "massive"). In the samples studied by DTA, several phases were detected, which could be identified using JCPDS databases [11] and other references [12]. The $x = 0$ sample, besides orthorhombic $FePO_4$ in heterosite form, contained also α-$FePO_4$ (a hexagonal quartz-like structure). The $x = 1$ sample was a mixture of $LiFePO_4$ in triphylite (orthorhombic) form and $Li_3Fe_2(PO_4)_3$ in monoclinic Nasicon-like form. In a case of the $x = 0.4$ sample (referred as "nano"), we also detected a mixture of triphylite and Nasicon-like phases. For that sample we additionally

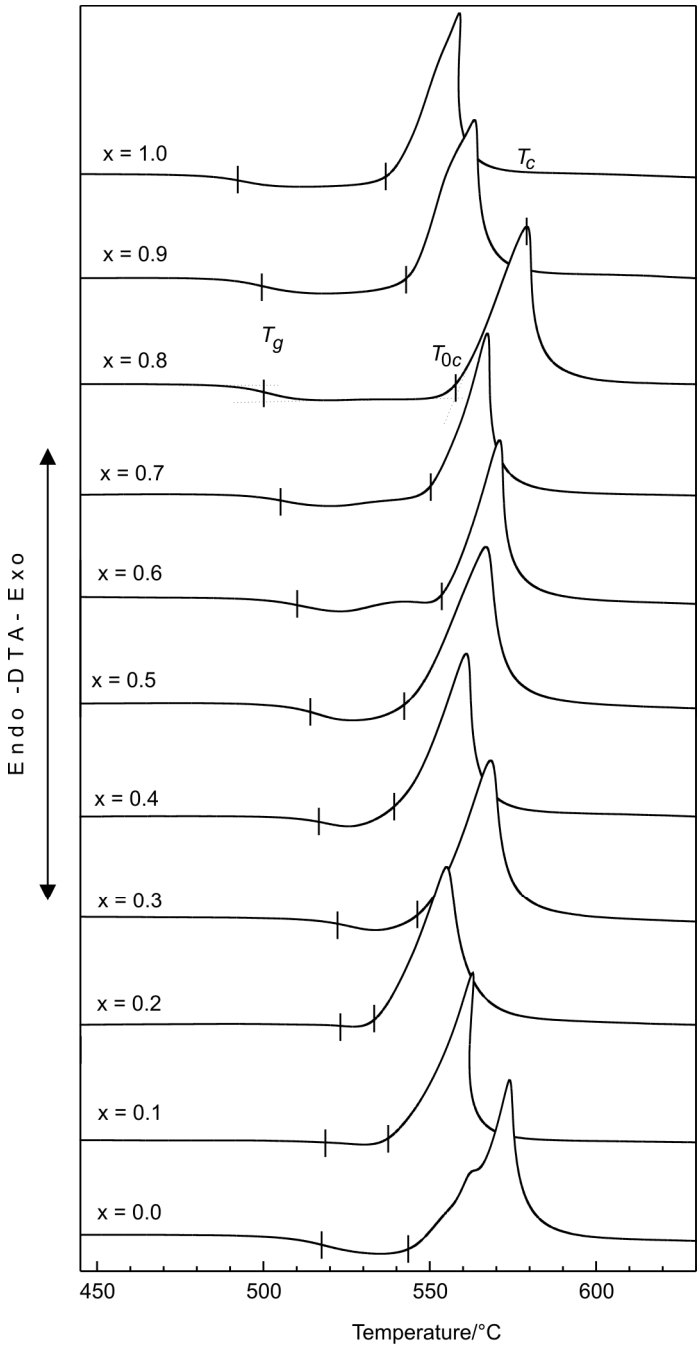

Fig. 1. Differential thermal analysis (DTA) runs
for glasses containing various amounts of lithium

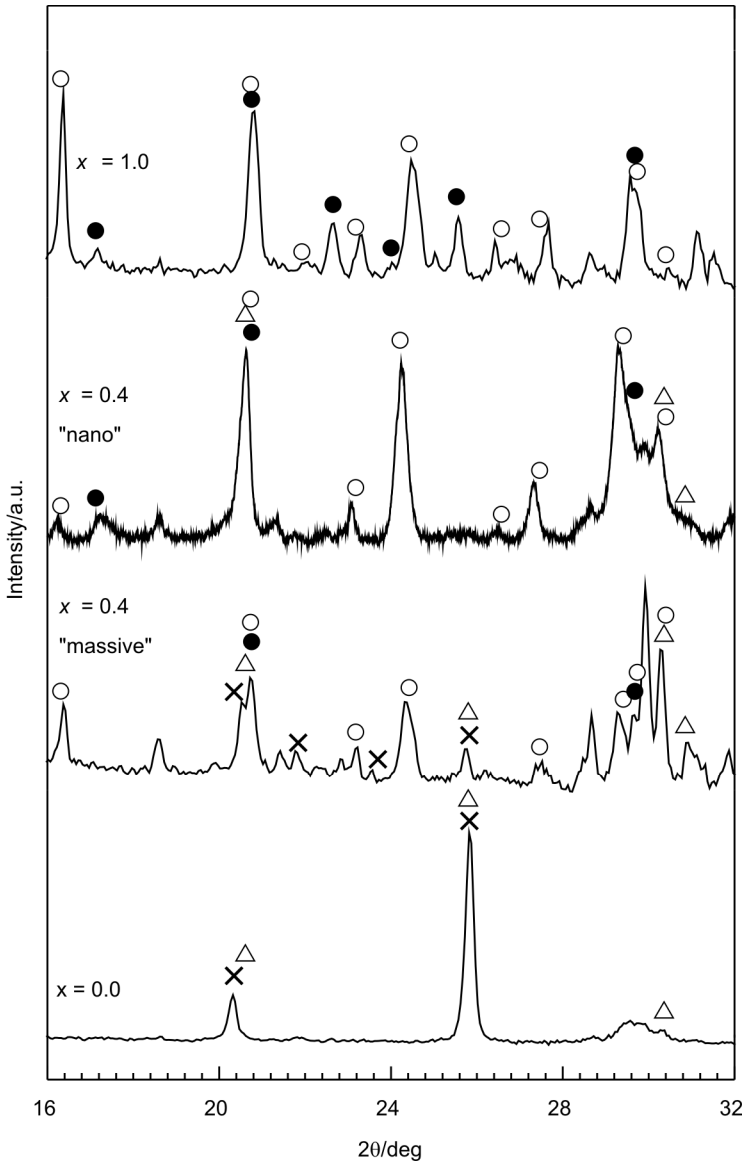

Fig. 2. Room temperature XRD patterns of samples of composition corresponding to: $x = 1$ (top curve), $x = 0.4$ "nano" (after nanocrystallization), $x = 0.4$ "massive" (after massive crystallization) and $x = 0$ (bottom curve). Symbols denote identified crystalline phases: full circles – $LiFePO_4$, open circles – $Li_3Fe_2(PO_4)_3$, triangles – $FePO_4$, crosses – α-$FePO_4$ [11, 12]

observed a broadening of XRD peaks. From the linewidth of the crystalline peaks it was possible to estimate, by a Scherrer formula, that the crystalline particles do not exceed 100 nm in size. Corresponding peaks were much better resolved in the case of

the sample after massive crystallization (Fig. 2). Additionally, in that case we also detected α-$FePO_4$ and heterosite phases.

3.2. Local structure

In order to determine the main features concerning the local structure of the glasses under study, a series of FTIR absorption measurements were carried out. The vibrational spectroscopic data are especially valuable in the case of amorphous systems, for which the natural method of structure determination – X-ray diffractometry – is ineffective.

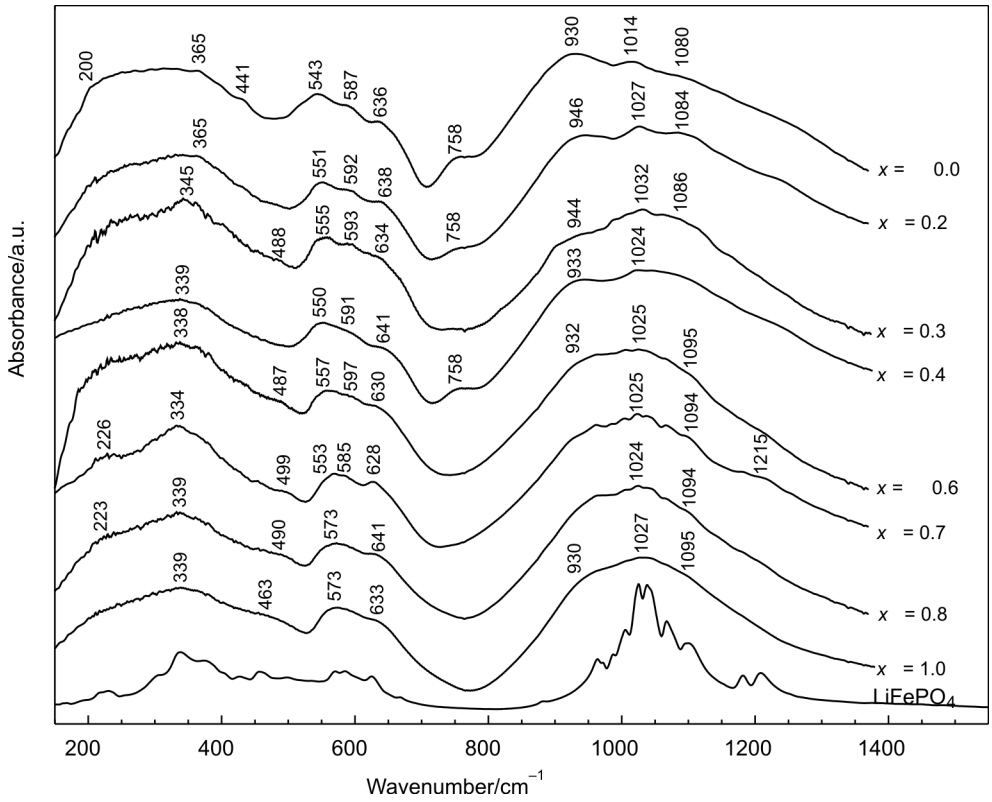

Fig. 3. FTIR absorption spectra of glasses containing various amounts of lithium (the bottom spectrum corresponds to crystalline $LiFePO_4$ [8])

Infrared absorption spectra of studied glassy materials are shown in Fig. 3 and compared with the IR spectrum of $LiFePO_4$ crystal reported in the literature [8, 9, 13–16]. There is a good agreement between the absorption bands of glasses measured in this work and the spectra of the $LiFePO_4$ crystalline phase [8, 16]. Broadening and overlapping of bands recorded for glasses is due to the much higher degree of disorder in

those systems in comparison with crystalline olivine phase. The spectra of the glasses under study can be divided into three wide features centred at about 1050, 600 and 350 cm^{-1}. These bands correspond to symmetric and asymmetric stretching oscillations of PO_4 units, bending oscillations of those units and lattice modes, respectively. Lattice modes (below 400 cm^{-1}) consist primarily of oscillations of oxygen, phosphorus and iron atoms. It is remarkable that, in a high wavenumber range, the IR bands appear exactly at the same positions as that for the crystalline phase. These patterns are consistent with the assumption that the PO_4 tetrahedra have very stable chemical bonds, even when they are the backbone of the vitreous phase. The bands in the spectral range 400–550 cm^{-1} (Li–O oscillations) are weakly dependent on the local lithium environment [9]. The mode at about 640 cm^{-1} is associated with FeO_6 vibrations. The fact that the mode is weaker and less resolved than those of PO_4 provides evidence that the FeO_6 octahedra are substantially disordered in the glasses. At a lower content of lithium ($0 \leq x \leq 0.4$) there are additional weak peaks at 758 cm^{-1} attributed to symmetric stretching vibrations of P–O–P bridging bonds in pyrophosphate $(P_2O_7)^{4-}$ units [17]. Their presence becomes more pronounced in the glasses of compositions which closely resemble $FePO_4$. It is noteworthy that the bands corresponding to the vibration of PO_4 units are almost independent of the lithium content. This indicates that the basic phosphate glass network remains insensitive to the presence of lithium ions.

3.3. Electrical properties

Generally, a lithium-free glass exhibits a typical impedance spectrum composed of a single semicircle characteristic of purely electronic (polaronic) conductors. Electronic conduction occurs via electron hopping between Fe^{2+} and Fe^{3+} ions, which serve as hopping centres for electrons [18]. Impedance spectra of glasses containing lithium consisted of a distorted semicircle, which may indicate phase heterogeneity of the samples or the influence of an ionic component (Li^+) of the total conductivity (strongly overlapped impedance semicircles). Very recent studies by Amin et al. [19] carried out on single crystals of $LiFePO_4$ have shown that the ionic component of electrical conductivity is much lower than the electronic one. Room temperature conductivity of the studied glasses, like in the case of their crystalline counterparts, is relatively low (ca. 10^{-7} $S \cdot cm^{-1}$ for the sample of $x = 1$). However at 450 °C it reaches 10^{-2} $S \cdot cm^{-1}$. The temperature dependences of conductivity for the glasses under study are in accordance with the Arrhenius formula (Fig. 4), with an effective activation energy E_a which slightly increases at about 180 °C. The lowest conductivity was found for the glass $FePO_4$ (not containing lithium). This is apparently due to the predominance of Fe^{3+} centres in such glass, resulting in the smallest concentration of Fe^{2+}–Fe^{3+} pairs essential for electronic hopping. For glasses containing lithium, the concentration of such aliovalent pairs is higher ($LiFePO_4$ introduces Fe^{2+} centres) and therefore their electronic conductivity is higher. Furthermore, those glasses exhibit an ionic component of total conductivity.

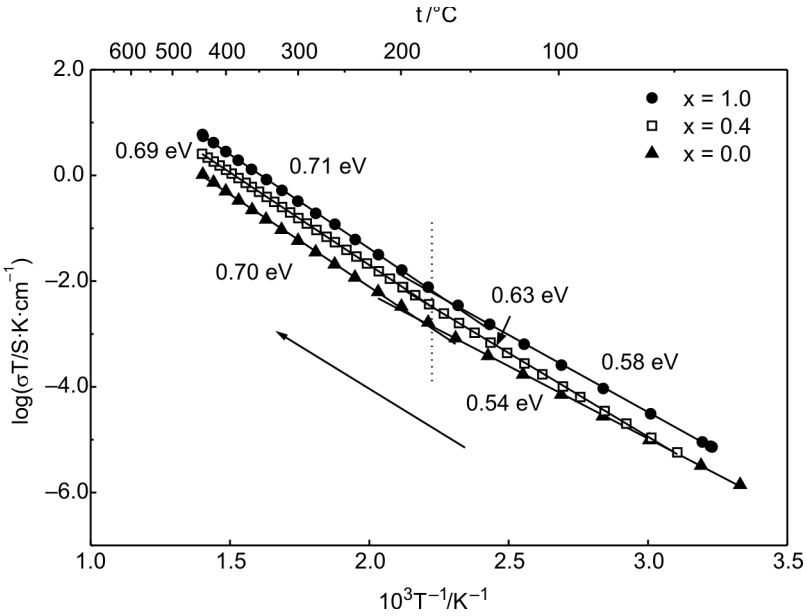

Fig. 4. Temperature dependences of conductivity for glassy samples with three different lithium contents (x = 0, 0.4 and 1)

The activation energies in the low temperature range (up to 180 °C) are equal to: 0.54, 0.63 and 0.58 eV for the glass of compositions corresponding to: $x = 0$, 0.4 and 1, respectively. It is interesting to note that those values are comparable to activation energies obtained for various crystallographic axes in anisotropic single crystal of $LiFePO_4$ [19]. Above 180 °C, the activation energies are almost independent of composition and are equal to about 0.70 eV (Fig. 4).

3.4. Electrical properties after nanocrystallization

In order to explore a possibility of improving the electrical conductivity of the samples under study by thermal treatment, we carried out electrical measurements at temperatures ranging from room temperature up to the temperature T_{0c} , corresponding to the beginning of the crystallization. Then we cooled the samples down to room temperature. The electrical conductivity of the $x = 0$ sample reaches its maximum value of 2×10^{-3} S·cm^{-1} at T_{0c} = 540 °C (Fig. 5). On cooling, the conductivity is systematically higher than that on heating, especially at lower temperatures. The increase in the conductivity at room temperature is about one order of magnitude. Also, the activation energies on cooling are different (lower) from those observed on heating. This increase of conductivity was confirmed on repeated heating-cooling cycles performed for some samples. After consecutive heating – cooling cycles there was a further slight increase in the conductivity. The observed changes can be explained based on SEM micrographs. The microstructure of the $x = 0$ sample, after its heating up to

temperature of the beginning of the crystallization, is shown in Fig. 6. The sample is only partly crystallized, with a substantial share of the amorphous phase still present.

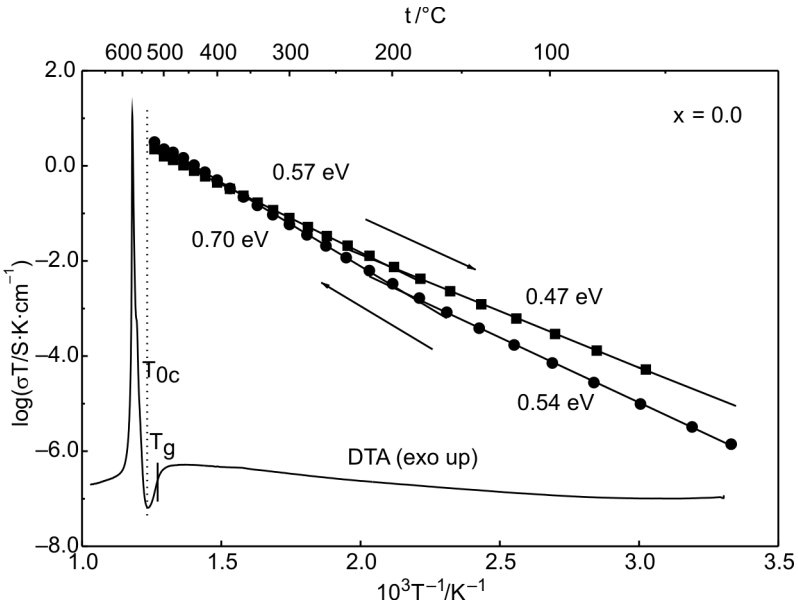

Fig. 5. Temperature dependences of conductivity during heating and cooling for a sample of $x = 0$ combined with DTA run of that sample during heating

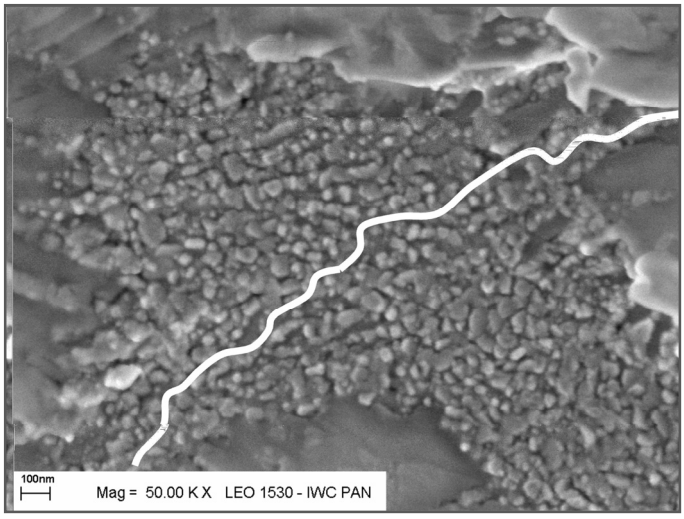

Fig. 6. Scanning electron microscopy (SEM) micrograph of the sample described by $x = 0$ after annealing at T_{0c} = 540 °C. The white line between nanocrystallites depicts an easy conduction path

The heterogeneity of the thermally treated samples may be a cause of the change of the activation energy of the sample on cooling from 0.57 eV above ca. 220 °C to

0.47 eV below that temperature. In Figure 6, one can see a number of isolated nanocrystallites embedded in the glassy matrix. Average grain size does not exceed 100 nm, which corresponds well with the estimates from XRD linewidth analysis. The interface regions between nanocrystallites and amorphous phase are, in our opinion, crucial for the observed conductivity enhancement and the decrease in the activation energy values. One can expect that in the highly defective interfacial regions, the concentration of Fe^{2+}–Fe^{3+} pairs, essential for the electron hopping, would be higher than inside crystallites and within the glassy phase. The density of the interfaces is high enough to form "easy conduction paths" whose conductivity is higher than that of the crystallites and that of the bulk glassy phase. A similar effect, namely a substantial increase in conductivity after nanocrystallization, was observed by us for glasses of the Li_2O–V_2O_5–P_2O_5 system [10].

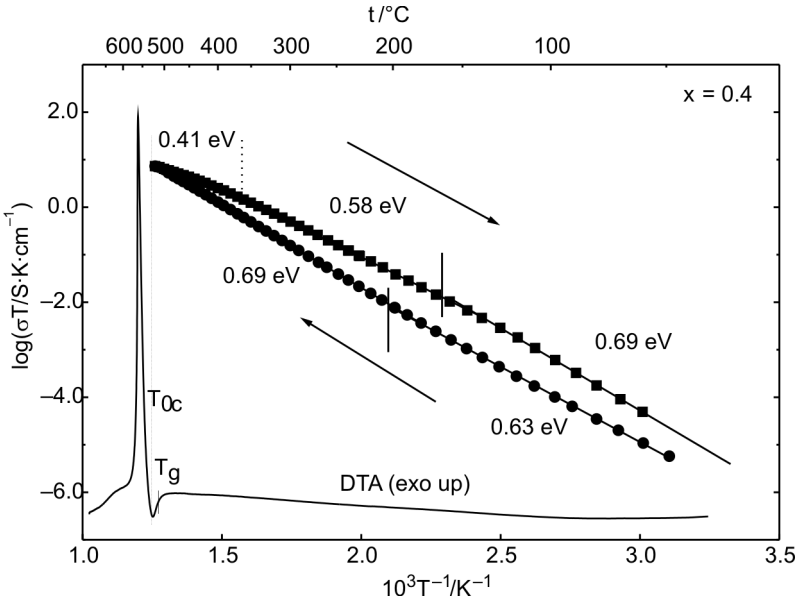

Fig. 7. Temperature dependences of conductivity during heating and cooling for a sample of $x = 0.4$ combined with DTA run of that sample during heating

The temperature dependence of conductivity of the sample corresponding to $x = 0.4$ heated up to $T_{0c} = 530$ °C is shown in Fig. 7. It can be seen that on the cooling run, the conductivity is systematically higher than that on the heating run. The maximum values of the electrical conductivity equal to 1.1×10^{-2} S·cm^{-1} were observed at 530 °C. The conductivity at room temperature of the samples heated up to T_{0c} and cooled down for this sample was increased by factor of 4 from the initial values. This enhancement was due to the nanocrystallization phenomena taking place at temperature T_{0c}. The observed irreversible increase in conductivity is accompanied by a change in the activation energies observed in the cooling stage. The activation ener-

gies start from 0.41 eV in the temperature range 360–530 °C, increase to 0.58 eV in the 160–360 °C range and reach 0.69 eV below 160 °C (Fig. 7). The observed increase of the activation energy values can be attributed to a possible ordering of the emerged crystalline phases. It is known [12] that at temperatures higher than 350 °C crystalline olivines $FePO_4$ and $LiFePO_4$ form solid solutions (disordered phase D). At temperatures lower than 200 °C there are two separate phases: H (heterosite) and T (triphylite). In the intermediate temperature range (200–350 °C) both H and D phases coexist. A similar situation of ordering and separation of the crystalline phases taking place on cooling can occur in our partly crystallized samples. In the case of the composition corresponding to $x = 0.4$, the situation is additionally complicated by the presence of a Nasicon-like phase and residuals of the glassy phase.

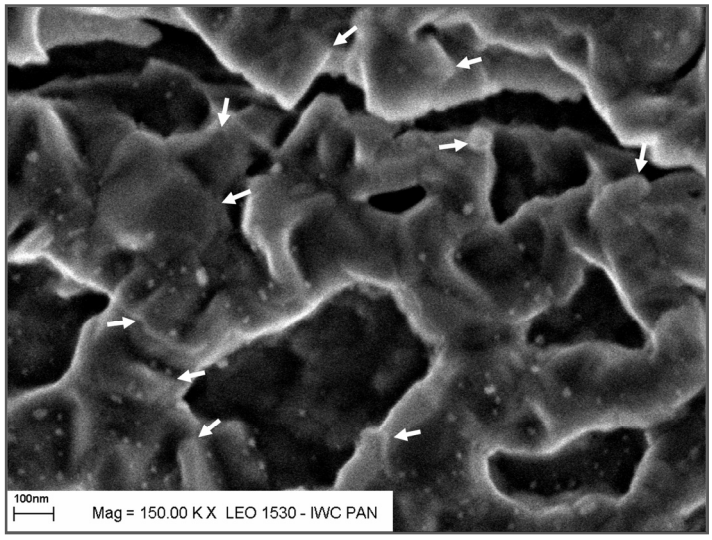

Fig. 8. SEM micrograph of the sample described by $x = 0.4$ after annealing at T_{0c} = 530 °C for 0.5 h (arrows show orthorhombic nanocrystallites of re-crystallized glass)

In a SEM micrograph showing a recrystallized region of that sample (Fig. 8) there are visible orthorhombic crystallites (probably triphylite) of approximate size 100 nm embedded in the remaining glassy phase. Both SEM micrographs (Figs. 6 and 8) reveal the substantial porosity of the samples under study after their nanocrystallization. Such porosity and considerable share of nanocrystalline grains in the samples may be useful for eventual application of studied materials as cathodes in lithium batteries.

4. Conclusions

The studies presented here of lithium-iron phosphate (LFP) glasses were, to the best of the authors' knowledge, the first to have been carried out on this subject.

Thermal stability and the local structure are weakly dependent on the composition (lithium content). LFP glasses exhibit mixed electronic-ionic conductivity, with the electronic component predominating. The conductivity reaches its maximum value of 10^{-2} S·cm^{-1} at 450 °C. This work has shown that the re-crystallization of LFP glasses at the nanoscopic scale can be carried out and that it does lead to a significant enhancement in the conductivity. Nanocrystallization seems to be the way ahead for electrical conductivity enhancement of amorphous lithium-iron phosphates.

Acknowledgements

The authors are grateful to Dr. S. Gierlotka, Institute of High Pressure Physics, Polish Academy of Sciences, for the assistance in SEM studies.

References

[1] MANTHIRAM A., GOODENOUGH J.B., J. Solid State Chem., 71 (1987), 349.
[2] PADHI A.K., NANJUNDASWAMY K.S., J.B. GOODENOUGH, J. Electrochem. Soc., 144 (1997), 1188.
[3] ZAGHIB K., STRIEBEL K., GUERFI A., SHIM J., ARMAND M., GAUTHIER M., Electrochim. Acta, 50 (2004), 263.
[4] BYKOV A.B., CHIRKIN A.P., DEMYANETS L.N., DORONIN S.N., GENKINA E.A., IVANOV-SHITS A.K., KONDRATYUK I.P., MAKSIMOV B.A., MELNIKOV O.K., MURADYAN, L.N., SIMONOV V.I., TIMOFEEVA V.A., Solid State Ionics, 38 (1990), 31.
[5] HUANG H., YIN S.C., NAZAR L.F., Electrochem. Solid-State Lett., 4 (2001), A170.
[6] CHEN Z., DAHN J.R., J. Electrochem. Soc., 149 (2002), A1184.
[7] CHUNG S.-Y., BLOKING J.T., CHIANG T.-M., Nature Mater., 1 (2002), 123.
[8] SALAH A.A., JOZWIAK P., ZAGHIB K., GARBARCZYK J.E., GENDRON F., MAUGER A., JULIEN C.M., Spectrochim. Acta, A 65 (2006), 1007.
[9] JOZWIAK P., GARBARCZYK J., GENDRON F., MAUGER A., JULIEN C.M., Mat. Res. Soc. Symp. Proc. 972 (2007), 6.
[10] GARBARCZYK J.E., „JOZWIAK P., WASIUCIONEK M., NOWINSKI J.L., J.„Power Sources, 173 (2007), 743.
[11] *JCPDS database of crystallographic data* (reference codes: $LiFePO_4$ - 00-040-1499, $Li_3Fe_2(PO_4)_3$ – 00-047-0107, α-$FePO_4$ – 01-077-0094).
[12] DODD J.L., YAZAMI R., FULTZ B., Electrochem. Sol. St. Lett., 9 (2006), A151.
[13] PAQUES-LEDENT M.T., TARTE P., Spectrochim. Acta, A 30 (1973), 673.
[14] SALAH A.A., JOZWIAK P., GARBARCZYK J., BENKHOUJA K., ZAGHIB K., GENDRON F., JULIEN C.M., J. Power Sources, 140 (2005), 370.
[15] BURBA C.M., FRECH R., J. Electrochem. Soc., 151 (2004), A1032.
[16] JOZWIAK P., GARBARCZYK J., GENDRON F., MAUGER A., JULIEN C.M., J. Non-Cryst.Solids, 354 (2008), 1915.
[17] NYQUIST R.A., PUTZIG C.L., LEUGERS M.A., *Infrared and Raman Spectral Atlas of Inorganic Compounds and Organic Salts: Raman Spectra*, Academic Press, San Diego, 1997.
[18] MOTT N.F., Adv.Phys., 50 (2001), 865.
[19] AMIN R., BALAYA P., CHEN D.P., LIN C.T., MAIER J., *16th International Conference on Solid State Ionics*, Shanghai, China, July 1- 6, 2007, Book of Program and Abstracts, p. 57.

Received 7 March 2008
Revised 30 January 2009